

Store-operated calcium entry is essential for glial calcium signalling in CNS white matter

M. Papanikolaou¹ · A. Lewis¹ · A. M. Butt¹

Received: 14 November 2016 / Accepted: 27 January 2017 / Published online: 28 February 2017
© The Author(s) 2017. This article is published with open access at Springerlink.com

Abstract ‘Calcium signalling’ is the ubiquitous response of glial cells to multiple extracellular stimuli. The primary mechanism of glial calcium signalling is by release of calcium from intracellular stores of the endoplasmic reticulum (ER). Replenishment of ER Ca^{2+} stores relies on store-operated calcium entry (SOCE). However, despite the importance of calcium signalling in glial cells, little is known about their mechanisms of SOCE. Here, we investigated SOCE in glia of the mouse optic nerve, a typical CNS white matter tract that comprises bundles of myelinated axons and the oligodendrocytes and astrocytes that support them. Using quantitative RT-PCR, we identified Orai1 channels, both Stim1 and Stim2, and the transient receptor potential M3 channel (TRPM3) as the primary channels for SOCE in the optic nerve, and their expression in both astrocytes and oligodendrocytes was demonstrated by immunolabelling of optic nerve sections and cultures. The functional importance of SOCE was demonstrated by fluo-4 calcium imaging on isolated intact optic nerves and optic nerve cultures. Removal of extracellular calcium ($[\text{Ca}^{2+}]_o$) resulted in a marked depletion of glial cytosolic calcium ($[\text{Ca}^{2+}]_i$), which recovered rapidly on restoration of $[\text{Ca}^{2+}]_o$ via SOCE. 2-aminoethoxydiphenylborane (2APB) significantly decreased SOCE and severely attenuated ATP-mediated calcium signalling. The results provide evidence that Orai/Stim and TRPM3 are important components of

the ‘calcium toolkit’ that underpins SOCE and the sustainability of calcium signalling in white matter glia.

Keywords Store-operated calcium channel · CRAC · TRP channel · Glia · Astrocyte · Oligodendrocyte · White matter · Calcium signalling

Introduction

Glial cells respond to a wide range of extracellular stimuli, including neurotransmitters, by a rise in cytosolic calcium ($[\text{Ca}^{2+}]_i$) termed ‘ Ca^{2+} signalling’, which is the basis of ‘glial excitability’ (Khakh and McCarthy 2015). Glial calcium signalling regulates the release of ‘gliotransmitters’, such as ATP, which couple glia within a panglial syncytium and act on neurones and cerebral vasculature to modulate neuronal activity and cerebral blood flow, with important roles in regulating glial physiological functions and pathology (Butt et al. 2014; Fern et al. 2014). Glial calcium signalling is mainly dependent on inositol 1,4,5-triphosphate (IP3)-mediated release of Ca^{2+} from the endoplasmic reticulum (ER), which depends on the replenishment of intracellular stores through store-operated calcium entry (SOCE) (Verkhatsky and Parpura 2014). The two main plasmalemmal channels mediating SOCE are transient receptor potential (TRP) channels, comprising six subfamilies, and calcium release-activated calcium channels (CRAC), which are formed of Orai, the plasmalemma spanning channels and STIM (Stromal Interaction Molecule), which function as ER Ca^{2+} sensors (Verkhatsky and Parpura 2014). Depletion of ER Ca^{2+} triggers STIM to interact with plasmalemmal SOCE channels, both Orai and TRP (Huang et al. 2006; Mercer et al. 2006), resulting in influx of Ca^{2+} from the extracellular milieu into

A. M. Butt and A. Lewis contributed equally to this work.

✉ A. M. Butt
arthur.butt@port.ac.uk

¹ Institute of Biomedical and Biomolecular Sciences, School of Pharmacy and Biomedical Science, University of Portsmouth, Portsmouth PO1 2DT, UK

the cytosol and subsequent refilling of ER stores through uptake via calcium (SERCA) pumps on the ER membrane (Jousset et al. 2007). SOCE has been reported in astrocytes (Golovina 2005; Pivneva et al. 2008) and oligodendrocytes (Hoffmann et al. 2010) and, although the molecular mechanisms have not been fully resolved, it has been generally considered that astrocytes and oligodendrocytes depend mainly on TRP channels, whilst Orai are the predominant mechanism in microglia (Verkhatsky and Parpura 2014). In this study, we show that astrocytes and oligodendrocytes express both Orai/Stim and TRP channels in the mouse optic nerve, a typical CNS white matter tract.

White matter comprises bundles of myelinated axons and the glia that support them, ensuring the rapid communication between the different parts of the CNS that underlies the massive computing power of the brain (Butt et al. 2014). Hence, disruption of white matter, such as occurs in the demyelinating disease multiple sclerosis (MS), has devastating effect on CNS function (Fern et al. 2014). Despite the lack of neuronal cell bodies and synapses in white matter, neurotransmitter signalling is prominent and mediates axon–glial communication, which evokes Ca^{2+} signalling in astrocytes and oligodendrocytes and serves to couple their homeostatic and myelinating functions to axonal activity, thereby ensuring rapid electrical conduction (Butt et al. 2014). A key feature in CNS white matter glia is the predominance of ATP-mediated IP₃-dependent Ca^{2+} signalling, which has a clearly established role in glial physiology and pathology, including MS, stroke and traumatic injury (Rivera et al. 2016; Langer et al. 2017). However, despite the prominence of Ca^{2+} signalling in CNS white matter, the molecular mechanisms of SOCE have not been fully resolved. Here, we show that the SOCE channels TRPM3 and Orai/Stim are expressed by astrocytes and oligodendrocytes in the mouse optic nerve, and SOCE is shown to be essential for glial Ca^{2+} calcium signalling in this typical white matter tract.

Materials and methods

Experimental animals

All animals were killed humanely by cervical dislocation, in accordance with regulations issued by the Home Office of the UK under the Animals (Scientific Procedures) Act, 1986. The animals used were C57BL/6/10 wild type (WT) or PLP-DsRed transgenic mice, in which DsRed is under the control of the oligodendrocyte-specific proteolipid protein (PLP) promoter (Hirrlinger et al. 2005), kindly provided by Frank Kirchhoff (Molecular Physiology, University of Saarland, Homburg, Germany). Optic nerves were dissected free and placed immediately in either: (1) Buffer

RLT (Qiagen) for RNA extraction and qRT-PCR; (2) dissecting medium for explant cultures; (3) 41% paraformaldehyde (PFA) for immunohistochemistry; or (4) artificial cerebrospinal fluid (*a*CSF) for calcium imaging (details below).

qRT-PCR

Maintaining strict RNase-free and sterile conditions throughout, RNA extraction was performed using published protocols (Azim et al. 2014). RNA was processed using an RNeasy Micro kit (Qiagen) and converted to single-stranded cDNA using the RT² First Strand Kit (Qiagen), following manufacturer's instructions. The quantity of RNA that was transcribed was the same for all samples (500 ng). cDNA libraries were prepared from total RNA extracted from 10 pooled optic nerves from WT postnatal mice [aged postnatal day (P)9–12], and adult mice (aged P30–40), and analyses were run in triplicate. SYBR Green qPCR Mastermix (Qiagen) was mixed with cDNA and ultra-pure water (Ambion) and 25 μ l was pipetted in each well of the 96 well-plate arrays for the Lightcycler 96 (Roche), using the Mouse Neuronal Ion Channels RT² Profiler™ qPCR array and a custom RT² Profiler™ qPCR array for additional channels not included in the neuronal array, namely STIM1, STIM2, IP3R1, IP3R2, TRPC2, TRPM3, TRPM4, TRPM7 and TRPV1 (Sabiosciences, Qiagen). Relative gene expression was determined using the $2^{-\Delta C_t}$ method versus GAPDH which was identified as the most appropriate housekeeping gene using the Normfinder algorithm and the standard deviation (SD) method. Gene expression data are presented as mean \pm SEM, and samples compared for significance using ANOVA and unpaired *t* tests in Prism 6.0 (Graphpad).

Optic nerve explant cultures

Optic nerve explant cultures were prepared from mice aged postnatal day (P)7–12, as described previously (Greenwood and Butt 2003). In brief, optic nerves were carefully dissected and maintained in pre-warmed (37 °C) and pre-gassed (95% O₂/5% CO₂) dissecting media, consisting of high glucose Dulbecco's modified Eagle medium (DMEM) (Sigma-D5671) containing 10% foetal calf serum (Life Technologies), L-glutamine (Sigma) and 0.1% gentamycin (Life Technologies). From this point on optic nerves were kept under sterile conditions and cut into 1–2 mm fragments in filter sterilized pre-warmed dissecting media, using a scalpel blade. For further dissociation, optic nerve fragments were triturated and transferred onto poly-D-lysine/matrigel-coated coverslips. After 24 h, the dissecting medium was replaced with a low serum (0.5%) modified Bottenstein and Sato (B&S) culture medium (Bottenstein

and Sato 1979), supplemented with 10 ng/ml recombinant human PDGF-AA (R&D Systems) and 0.1% gentamicin. After 3–4 days *in vitro* (DIV) the medium was replaced with maturation medium, B&S media supplemented with 0.5 mM dibutyryl cAMP, for up to 12 DIV, changing media every 3–5 days. Explant cultures were used for immunolabelling or calcium imaging after maturation at 8–12 DIV, equivalent to \geq P20.

Immunolabelling

Optic nerve tissue and explant cultures were fixed in 1% paraformaldehyde in phosphate buffered saline (PBS, pH 7.4); tissue and explant cultures were fixed for 1 h and 10 min, respectively, at room temperature (RT), followed by washes in PBS. For sectioning, optic nerves from P15 PLP1-DsRed or WT mice were placed in cryoprotectant (30% wv⁻¹ sucrose in PBS) overnight at 4 °C, then embedded in Cryo-M-Bed (Bright Instruments Company Ltd), before rapidly freezing at –80 °C until use. Longitudinal optic nerve sections (14 μ m) were cut with a Leica CM3050 S cryostat at –21 °C and sections were transferred onto Polysine[®] coated slides (Thermo-Scientific). After this, tissue sections and cultures were treated the same. Following washes in PBS for 30 min, a blocking stage was performed using 5% normal goat serum (NGS) in PBS for 1 h at RT; where primary antibodies targeted an intracellular epitope, Triton X-100 (Sigma) was included in the blocking solution (0.1% for tissue sections and 0.01% for cultured cells). Primary antibodies were diluted in blocking solution and tissues/cells incubated overnight at 4 °C; anti-STIM1, anti-STIM2, anti-ORAI1, anti-TRPM3 were raised in rabbits (Alomone) and used at 1:300; chicken anti-GFAP (Chemicon) was used at 1:500. Samples were then washed 3 times in PBS and incubated with the appropriate secondary antibodies conjugated with Alexafluor 488 or 568 (1:400, Life Technologies), DyLight[™] 649 (1:200, Stratech) or TRITC (1:100, Sigma); counterstaining with Hoechst Blue (1:1000, Fisher) was used to label cell nuclei. Controls were carried out in which sections/cells were pre-absorbed with antigen peptide overnight prior to incubation in the primary antibody. Following immunolabelling, coverslips/sections were mounted with Fluoromount-G[®] (Southern Biotech). Immunohistochemical labelling was determined by confocal microscopy, based on 2–3 sections for each antibody from $n=3$ optic nerves, or from $n=3$ coverslips for explant cultures.

Image capture and analysis

Immunofluorescence was detected using excitation wavelengths of 488 nm (green), 568 nm (red), 633 nm (far red) and 405 nm (blue), with an argon, HeNe1 and diode laser,

respectively. Confocal images were captured using the 20 \times or 40 \times oil immersion objectives, and images acquired using multi-track sequential capture, with optimal detector gain and offset acquisition settings for pinhole diameter 0.13–0.3 airy units, with an average of four scans per image, to detect positive signal with minimal background and prevent cross-talk between channels. Identical settings were used to image negative controls. *z*-stacks were captured of 4–15 *z*-sections (voxel size 43–76 nm *x*-*y*, 76–283 nm *z*). Image analysis was carried out using Volocity 6.1 software (PerkinElmer). For confocal photomicrographs, two-dimensional flattened images of the *z*-stacks are presented of representative data, from 2 to 3 sections for each antibody from $n=3$ optic nerves, or from $n=3$ coverslips for explant cultures. Colocalization images were obtained using Volocity 6.1 software, as described previously (Mondragao et al. 2016), by thresholding to separate the positive signal (positive immunolabelling) from background, using the negative controls, and calculating the thresholded Pearson's correlation coefficient (PCC) to generate a colocalization channel representing in three-dimensions the voxels in which the two channels overlap with the same intensity.

Calcium imaging

Optic nerves from P8-P13 PLP-DsRed and WT mice were isolated intact and placed in aCSF, comprising (in mM): NaCl 133, KCl 3, CaCl₂ 2.24, NaH₂PO₄ 1.2, MgCl₂ 1.0, D-glucose 10, HEPES 8.55, pH 7.3. For calcium imaging, nerves or cultures of optic nerve glia were incubated in aCSF containing 4 μ M Fluo-4/AM for 60 min at RT, as described previously (Hamilton et al. 2008). Fluo-4 loaded samples were transferred to a perfusion chamber under a Zeiss LSM510 Pascal Axioskop 2 confocal microscope and imaged using a 20 \times /0.50 WPh2 Achromplan water immersion lens. Fluo-4 was excited with 488 nm argon laser and emitted light was collected at 510–580 nm. A series of optical *z*-sections were collected, typically 7–8 sections at 2–3 μ m intervals, every 350–700 ms, and analysed using the Zeiss LSM Image Examiner software (Zeiss, Germany). Glial cell bodies were selected as regions of interest (ROI) and changes in fluorescence intensity above baseline ($\Delta F/F$) were measured in arbitrary units (AU). Data were expressed as mean \pm standard error of the mean (SEM), where 'n' represents the number of cells, and experiments were repeated a minimum of 3 times ($n=3$ nerves or coverslips); significance was determined by unpaired *t* tests, using Prism 6.0 (Graphpad). The tissues were continuously perfused via a multitap system that allowed rapid turnover of solutions. Pharmacological agents were dissolved directly in aCSF: ATP (Sigma, 100 μ M), which evokes raised cytosolic Ca²⁺ in astrocytes and oligodendrocytes mainly via P2Y receptors and is a reliable indicator

of cell viability (James and Butt 2001); the potent sarcoplasmic reticulum Ca^{2+} ATPase (SERCA pump) blocker thapsigargin (Tocris, 2–10 μM), which has been shown to cause influx of calcium into the cytosol due to intracellular calcium store depletion in glial cells (Gudz et al. 2006; Simpson and Russell 1997); and 2APB (Tocris, 50 μM), which blocks a range of TRP channels, including TRPM3, together with TRPC1, TRPC3, and TRPM7, and has been shown to abolish Ca^{2+} influx due to SOCC in astrocytes (Mandal et al. 2008). Calcium-free *a*CSF (ZERO-Ca^{2+}) was prepared by removal of CaCl_2 , addition of the Ca^{2+} -chelator 1 mM EGTA, and increasing HEPES to 10 mM to maintain osmolarity. Unless otherwise stated, ATP was applied by perfusion over the nerve for 60 s at the beginning and end of experiments, to confirm integrity of the cells, and a recovery period of 10 min in *a*CSF was allowed between tests pulses.

Results

Astrocytes and oligodendrocytes express Orai/Stim

To determine gene expression profiles of the main SOCE channels in postnatal and adult mice, we used qRT-PCR and normalized transcript levels against the housekeeping gene GAPDH by the comparative $2^{-\Delta\text{Ct}}$ method (Fig. 1); data are from ten pooled WT optic nerves in each age group, run in triplicate, with data expressed as mean \pm SEM ($n=3$). The results indicate that IP3 receptor 2 (IP3R2) is the primary ER Ca^{2+} release channel in optic nerve glia, with significantly lower expression of IP3R1 ($p<0.01$,

unpaired *t* test), whilst ryanodine receptor 3 (RyR3) was barely detectable; RyR3 is the main subtype expressed in the brain and RyR1 and RyR2 were not included in the Mouse Neuronal Ion Channels RT² Profiler™ assay. Notably, all three Orai isoforms and both Stim1 and Stim2 were detected in the optic nerve (Fig. 1). Orai1 was the most highly expressed isoform in the postnatal optic nerve ($p<0.05$, ANOVA) and levels of Orai1 were significantly lower in the adult nerve ($p<0.05$, unpaired *t* test). There were no statistically significant differences in transcript levels of the three Orai isoforms in the adult nerve, or between Stim1 and Stim2 in postnatal or adult nerves (Fig. 1).

Immunolabelling was performed in optic nerve sections and explant cultures from PLP-DsRed mice to identify oligodendrocytes (Fig. 2) and from WT mice using GFAP immunolabelling to identify astrocytes (Fig. 3); in both mouse strains the pattern of immunostaining was the same for Orai (Figs. 2a_{ii}, 3a_{ii}), Stim1 (Figs. 2b_{ii}, 3b_{ii}) and Stim2 (Figs. 2c_{ii}, 3c_{ii}). No immunoreactivity was detected in negative controls following preabsorption with the antigen peptide for each of the primary antibodies used (insets in Fig. 2a_{iii}, b_{iii}, c_{iii}). The most prominent expression of Orai1 in optic nerve sections was in rows of oligodendroglial cell somata identified by expression of the PLP-DsRed reporter (Fig. 2a_{i-iii}), which was confirmed by the generation of a colocalization channel that identifies the individual voxels in which the red (PLP-DsRed) and green (Orai1 immunostaining) channels overlap with the same intensity (Fig. 2a_{iv}), as described previously (Hawkins and Butt 2013). The results demonstrate clear colocalization of Orai1 with PLP-DsRed in oligodendroglial somata in optic nerve sections (Fig. 2a_{iv}), and the presence of

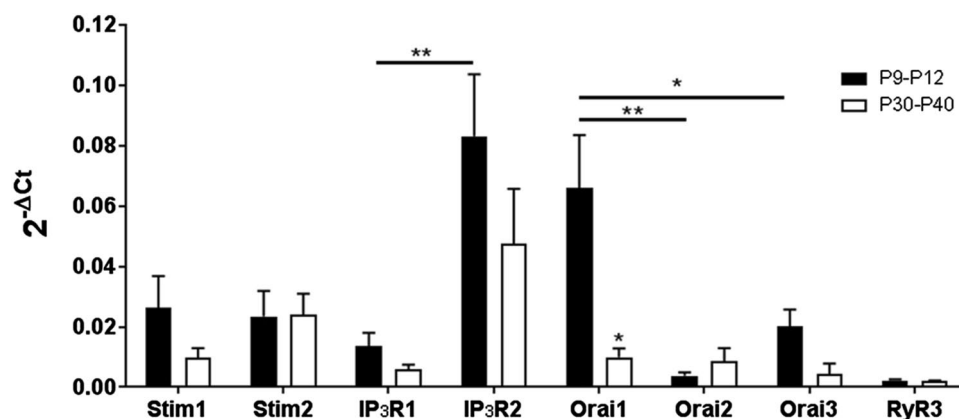


Fig. 1 Expression of Orai/Stim transcripts in the mouse optic nerve. qRT-PCR was performed on lysates of acutely isolated optic nerves from WT postnatal mice (aged P9–P12) and adult mice (P30–P40). Data are from ten pooled optic nerves in each age group, run in triplicate, expressed as relative mRNA levels ($2^{-\Delta\text{Ct}}$) compared to the housekeeping gene GAPDH (mean \pm SEM, $n=3$). Orai1 was the most highly expressed Orai isoform in the postnatal nerve ($*p<0.05$,

$**p<0.01$, ANOVA and unpaired *t* tests) and was significantly down-regulated with age ($*p<0.05$, unpaired *t* test); there was no significant difference between the Orai isoforms in the adult. There was no significant difference between Stim1 and Stim2 expression in postnatal or adult nerves. IP3R2 was expressed at significantly greater levels than IP3R1 at both ages ($**p<0.01$, unpaired *t* test); there was no significant difference between the age groups

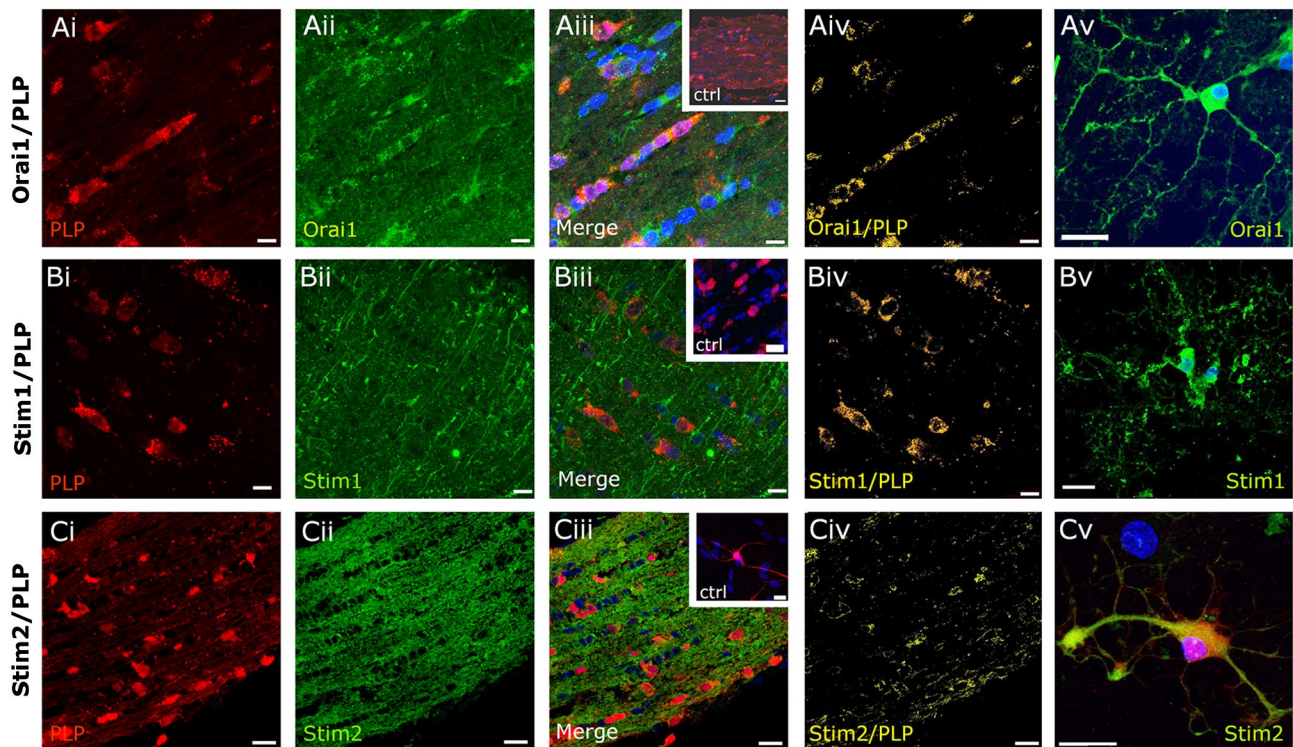


Fig. 2 Expression of Orai/Stim in optic nerve oligodendrocytes. Immunolabelling for Orai1 (**a**, green), Stim1 (**b**, green) and Stim2 (**c**, green) in PLP-DsRed mice to identify oligodendrocytes (**a–c**, red), in optic nerve sections (**ai–iv**, **bi–iv**, **ci–iv**) and explant cultures (**av**, **bv**, **cv**). Confocal micrographs illustrate single channels (**ai**, **aii**, **bi**, **bii**, **ci**, **cii**) and merged channels (**aiii**, **biii**, **ciii**). Expression of Orai1 and Stim1 is localized to oligodendroglial somata, whereas Stim2 immunostaining was primarily within the fascicles of myelinated axons,

as demonstrated by the colocalization channels, illustrating voxels in which green and red channels are of equal intensity and appear yellow (**aiv**, **biv**, **civ**). Oligodendrocytes in explant cultures are immunopositive for Orai1 (**av**), Stim1 (**bv**) and Stim2 (**cv**). No immunostaining was observed in negative controls that were pre-incubated in blocking peptides for Orai1 (*inset*, **aiii**), Stim1 (*inset*, **biii**) and Stim2 (*inset*, **ciii**). Nuclei are stained with Hoechst blue. Scale bars, **b** 10 μ m, **c** 20 μ m

Orai1 in oligodendrocytes is morphologically confirmed in optic nerve explant cultures (Fig. 2av). In addition, oligodendrocytes were immunopositive for Stim1 (Fig. 2bi–iii), which the colocalization channel indicates is strongest in oligodendroglial somata (Fig. 2biv). In contrast, Stim2 immunostaining was strongest within the myelinated axon fascicles between the rows of oligodendrocyte somata (Fig. 2ci–iii), and is observed to decorate oligodendroglial processes in the colocalization channel (Fig. 2civ). Oligodendroglial expression of Stim1 and Stim2 was morphologically confirmed in cultured cells (Fig. 2bv, cv). Double immunofluorescence labelling of WT optic nerve sections with GFAP showed that astrocytes are immunopositive for Orai1 and Stim1 (Fig. 3ai–iii, bi–iii), but they were immunonegative for Stim2 (Fig. 3ci–iii), which was confirmed by generation of a colocalization channel in sections (Fig. 3aiv, biv, civ) and morphologically in cell cultures (Fig. 3av, bv, cv). The results support the potential importance of Orai1/Stim1 CRAC in white matter astrocytes and oligodendrocytes.

TRPM3 are the main TRP channels in optic nerve astrocytes and oligodendrocytes

qRT-PCR transcriptomic analysis indicated that by far the most abundant TRP channel in the WT postnatal and adult optic nerve is TRPM3 (Fig. 4a, $p < 0.001$, ANOVA and post hoc unpaired t tests), which mediates Ca^{2+} entry in response to a variety of different stimuli, such as sphingolipids and extracellular osmotic disturbances (Hoffmann et al. 2010). Immunolabelling for TRPM3 was performed on optic nerve sections and explant cultures from WT mice using GFAP immunolabelling to identify astrocytes (Fig. 4b) and PLP-DsRed mice to identify oligodendrocytes (Fig. 4c); the pattern of TRPM3 immunostaining was similar in both strains (Fig. 4bii, cii), and no immunoreactivity was detected in negative controls following preabsorption with the antigen peptide for the TRPM3 primary antibody (insets in Fig. 4biii, ciii). Double immunofluorescence labelling for GFAP and TRPM3 shows for the first time that astrocytes express TRPM3 in optic nerve sections

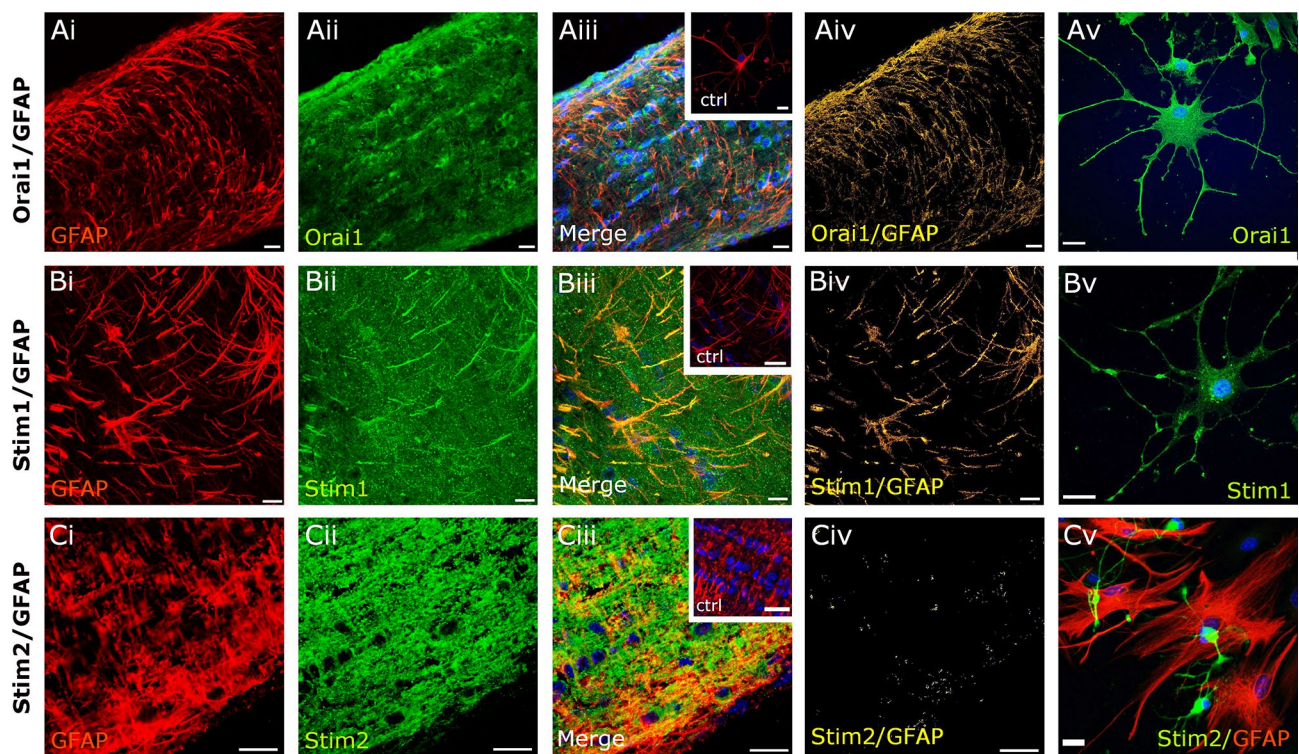


Fig. 3 Expression of Orai/Stim in optic nerve astrocytes. Double immunofluorescence labelling for Orai1 (**a**, *green*), Stim1 (**b**, *green*) and Stim2 (**c**, *green*), with GFAP to identify astrocytes (**a–c**, *red*), in WT optic nerve sections (**ai–iv**, **bi–iv**, **ci–iv**) and explant cultures (**av**, **bv**, **cv**). Confocal micrographs illustrate single channels (**ai**, **aii**, **bi**, **bii**, **ci**, **cii**) and merged channels (**aiii**, **biii**, **ciii**). Expression of Orai1 and Stim1 is localized to astrocyte processes, whereas astrocytes were immunonegative for Stim2, as demonstrated by the colocalization

channels, illustrating voxels in which *green* and *red* channels are of equal intensity and appear *yellow* (**aiv**, **biv**, **civ**). Astrocytes in explant cultures are immunopositive for Orai1 (**av**) and Stim1 (**bv**), but are immunonegative for Stim2 (**cv**). No immunostaining was observed in negative controls that were pre-incubated in blocking peptides for Orai1 (*inset*, **aiii**), Stim1 (*inset*, **biii**) and Stim2 (*inset*, **ciii**). Nuclei are stained with Hoechst blue. *Scale bars*, **b** 10 μm , **c** 20 μm

(Fig. 4bi–iii) and astrocytic expression is morphologically confirmed in optic nerve explant cultures (Fig. 4bv). Colocalization analysis of TRPM3 and GFAP immunostaining indicated TRPM3 is localized mainly to astrocyte processes (Fig. 4biv). In addition, TRPM3 is expressed in PLP-DsRed+ oligodendrocytes (Fig. 4ci–iii), in support of a previous study demonstrating TRPM3 in sphingosine-sensitive oligodendrocytes (Hoffmann et al. 2010). Generation of colocalization channels for PLP-DsRed and TRPM3 immunostaining indicates TRPM3 is highly localized to oligodendrocyte somata (Fig. 4civ), which is confirmed in cultured oligodendrocytes, where TRPM3 appeared to be excluded from distal oligodendroglial processes (Fig. 4cv). qRT-PCR indicated that other TRP channel subtypes included in the mouse neuronal array were expressed at much lower levels than TRPM3 (Fig. 4a). The second most expressed TRP channel transcript was TRPM7, followed by the ‘canonical’ TRPC1 and TRPV2, whereas TRPC3 and TRPM6 were expressed at low levels, and TRPA1, TRPV3, TRPV4, TRPM4 and TRPC6 were barely detectable, whilst TRPV1 and TRPM8 were not detected (Fig. 4a).

Functional SOCE in astrocytes and oligodendrocytes

SOCE was examined by fluo-4 calcium imaging in isolated intact optic nerves (Fig. 5a–c), using the SERCA pump blocker thapsigargin (10 μM) to induce depletion of ER Ca^{2+} stores and stimulate SOCE (Moreno et al. 2012), and 2APB (50 μM), which is a potent blocker of SOCE channels at high concentrations (Abdullaev et al. 2008; Singaravelu et al. 2006). No difference was found between WT and PLP-DsRed strains and the data were combined. Removal of extracellular $[\text{Ca}^{2+}]_o$ resulted in a depletion of glial cytosolic $[\text{Ca}^{2+}]_i$, which recovered rapidly on return to normal $[\text{Ca}^{2+}]_o$ (Fig. 5ai), due to Ca^{2+} influx across the plasmalemma from the extracellular milieu, as illustrated by the representative images (Fig. 5ai) and traces (Fig. 5bi) of changes in glial cytosolic $[\text{Ca}^{2+}]_i$ in the isolated intact optic nerve. The recovery in glial cytosolic $[\text{Ca}^{2+}]_i$ was markedly greater and sustained in the presence of thapsigargin, which blocked SERCA-mediated removal of Ca^{2+} from the cytosol into the ER stores (Fig. 5aii, bii). Conversely, blockade

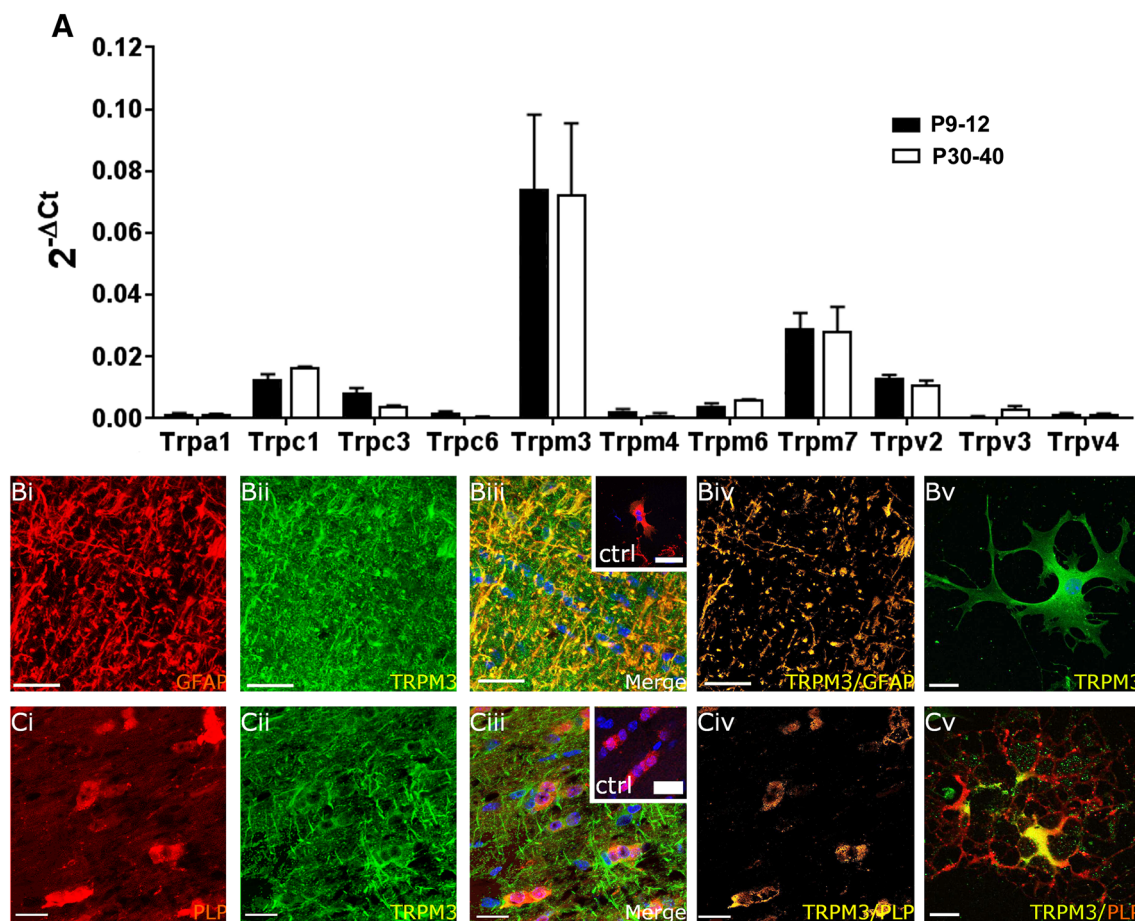


Fig. 4 Expression of TRP channels in optic nerve glia. **a** qRT-PCR of acutely isolated optic nerves from WT mice aged P9–P12 and P30–P40; data are from 10 pooled optic nerves in each age group, run in triplicate, expressed as relative mRNA levels ($2^{-\Delta C_t}$) compared to the housekeeping gene GAPDH method (mean \pm SEM, $n=3$). TRPM3 was the most highly expressed TRP channel in the postnatal and adult nerve ($***p<0.001$, ANOVA and unpaired t tests) and there was no developmental regulation of TRP channels, which had a rank order of expression in the adult of TRPM3 >>> TRPM7 ($***p<0.001$, unpaired t test) > TRPC1 ($*p<0.05$, unpaired t test) >> TRPV2 ($**p<0.01$, unpaired t test); TRPC3, TRPM6 and TRPV3 were expressed at significantly lower levels, and TRPA1, TRPC6, TRPM4, and TRPV4 were barely detectable. Immunolabeling for TRPM3 (**b**, **c**, green) with GFAP to identify astrocytes in WT

nerves (**b**, red) and in PLP-DsRed nerves to identify oligodendrocytes (**c**, red), in optic nerve sections (**bi–iv**, **ci–iv**) and explant cultures (**bv**, **cv**). Confocal micrographs illustrate single channels (**bi**, **bii**, **ci**, **cii**) and merged channels (**biii**, **ciii**). The colocalization channels illustrate voxels in which green and red channels are of equal intensity and appear yellow, showing expression of TRPM3 is localized to astroglial processes (**bv**) and oligodendroglial somata (**cv**). Immunostaining of explant cultures shows astrocytes are immunopositive for TRPM3 (**bv**) and that TRPM3 is localized to oligodendroglial somata and excluded from their distal processes (**cv**). No immunostaining was observed in negative controls that were pre-incubated in blocking peptides for TRPM3 (insets, **biii**, **ciii**). Nuclei are stained with Hoechst blue. Scale bars 20 μ m

of SOCE channels by a high concentration (50 μ M) of 2APB completely abolished the recovery in glial cytosolic $[Ca^{2+}]_i$, indicating replenishment of intracellular Ca^{2+} stores is entirely dependent on Ca^{2+} influx from the extracellular milieu via SOCE (Fig. 5a_{iii}, b_{iii}). Compared to controls ($n=81$ cells from 5 nerves), the effects of thapsigargin ($n=37$ cells from 3 nerves) and 2APB ($n=83$ cells from 5 nerves) were statistically significant (Fig. 5c, $p<0.001$, unpaired t tests with Welch's correction). It is difficult to distinguish unequivocally between astrocytes and oligodendrocytes in the isolated intact

optic nerve (Hamilton et al. 2008), hence we repeated the experiments on optic nerve explant cultures in oligodendrocytes and astrocytes identified by their differential expression of the oligodendroglial reporter PLP-DsRed (Brasko et al. 2017). The results demonstrate that the effects of thapsigargin (2 μ M) and 2APB (50 μ M) were equivalent in situ (Fig. 5c) and in vitro (Fig. 5d_i), and the same response was observed in both oligodendrocytes (Fig. 5d_{ii}) and astrocytes (Fig. 5d_{iii}); in all cases, the effects of thapsigargin and 2APB in vitro were significant compared to controls ($p<0.001$, unpaired t tests

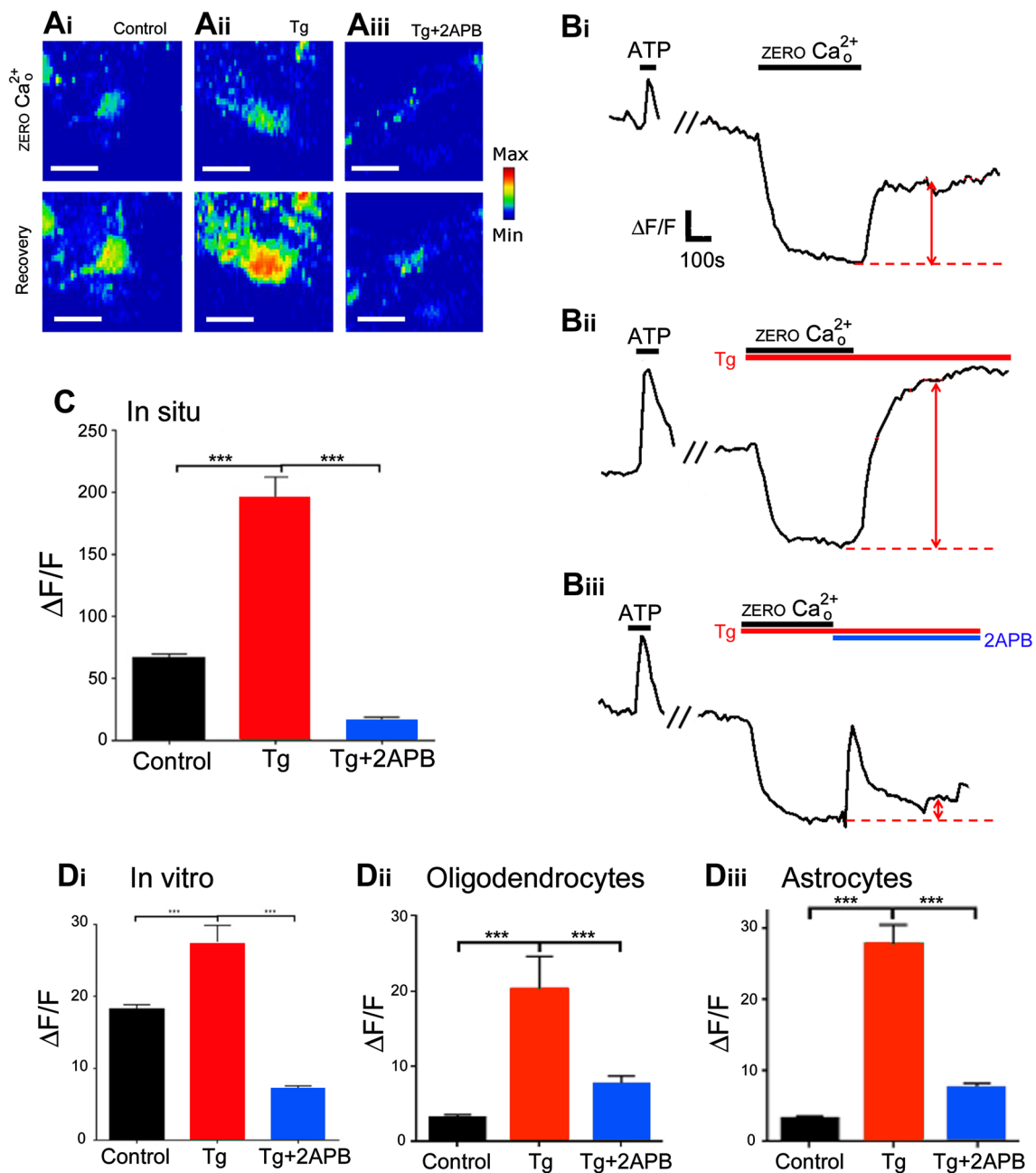


Fig. 5 SOCE in optic nerve glia. Mouse optic nerves were isolated intact and loaded with Fluo-4 to analyse SOCE, using thapsigargin (10 μ M for optic nerves, 2 μ M for explant cultures) to block ER reuptake and 2APB (50 μ M) to block SOCE channels. Confocal images of Fluo-4 fluorescence intensity illustrated in rainbow false colour (**a**, scale bars 10 μ m) and representative traces of individual glia (**b**), illustrating that removal of extracellular $[Ca^{2+}]_o$ results in a decline in cytosolic $[Ca^{2+}]_i$, which recovers rapidly on return to normal aCSF (**ai**, **bi**, red arrow), and this is markedly increased in the pres-

ence of thapsigargin (**aii**, **bii**, red arrow) and decreased in the presence of 2APB (**aiii**, **biii**, red arrow). Bar graphs showing the mean rise in cytosolic $[Ca^{2+}]_i$ (indicated by red arrows in **bi**–**biii**) in aCSF control, thapsigargin and 2APB, in situ in the isolated intact optic nerve (**c**) and in vitro in explant cultures (**d**), illustrating results from all glia (**di**) and separately for oligodendrocytes (**dii**) and astrocytes (**diii**), identified by differential expression of PLP-DsRed; data are mean \pm SEM change in fluorescence ($\Delta F/F$), *** p < 0.01, unpaired t test with Welch's correction

with Welch's correction: controls, $n=91$ cells from 3 coverslips; thapsigargin, $n=37$ cells from 3 coverslips; 2APB, $n=198$ cells from 5 coverslips). The results

demonstrate functional SOCE in white matter astrocytes and oligodendrocytes.

Notably, ATP-mediated calcium signals occur without decay following repeated applications of ATP and is the

primary mechanism of calcium signalling in optic nerve glia (James and Butt 2001). This was reaffirmed by consecutive administration of two test pulses of ATP for 60 s, with a 5-min recovery period between pulses (Fig. 6ai, ii), and there was no significant difference in the amplitude of the rise in glial cytosolic $[Ca^{2+}]_i$ between first and second pulses in control aCSF (Fig. 6b, $p > 0.05$, unpaired t test with Welch's correction; $n = 50$ cells from 3 nerves). In contrast, administration of thapsigargin to block replenishment of ER stores (Fig. 6aiii) or 2APB to block SOCE (Fig. 6aiv) resulted in a marked and statistically significantly attenuation in the response to the second application of ATP (Fig. 6b, $p < 0.001$ for thapsigargin ($n = 37$ cells from 3 nerves), $p < 0.01$ for 2APB ($n = 104$ cells from 6 nerves), unpaired t tests with Welch's correction). The results demonstrate that SOCE-dependent replenishment of ER Ca^{2+} stores is essential for ATP-mediated calcium signalling in optic nerve glia.

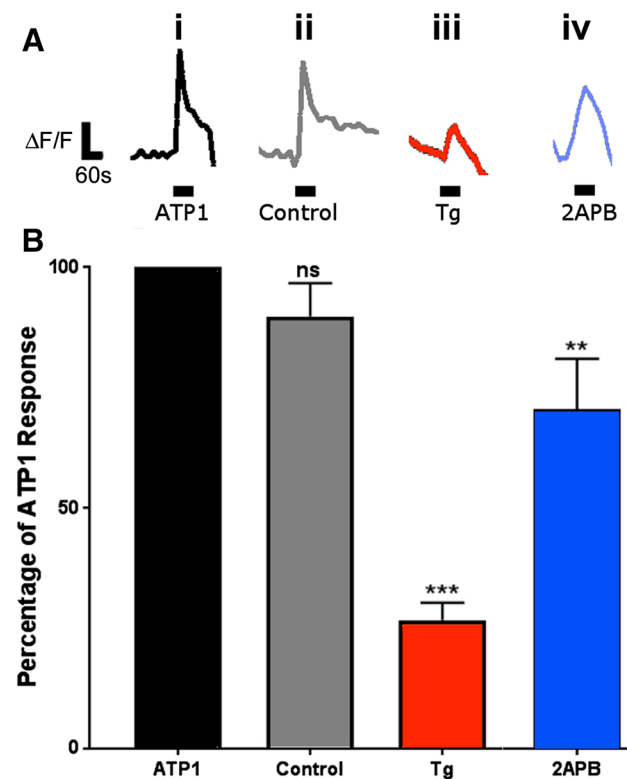


Fig. 6 SOCE is essential for sustainability of ATP-mediated Ca^{2+} signalling in optic nerve glia. **a** Representative traces illustrating ATP-mediated rise in glial Ca^{2+} at the beginning of each experiment (**ai**, ATP1) and the second response tested at the end of the experiment, without application of any pharmacological agents (**aii**, control), compared to after application of thapsigargin to block replenishment of ER Ca^{2+} stores (**aiii**, Tg), or 2APB to block SOCE (**aiv**, 2APB). **b** Bar graph of mean (\pm SEM) responses to the second test pulse of ATP, expressed as a percentage of the first response to ATP at the beginning of the experiment (** $p < 0.01$, *** $p < 0.001$, unpaired t tests with Welch's correction)

Discussion

Calcium signalling is a ubiquitous physiological characteristic of glial cells, but the mechanisms of Ca^{2+} replenishment that sustain glial calcium signalling are poorly understood. Here, we demonstrate that white matter astrocytes and oligodendrocytes in the mouse optic nerve express Orai/Stim as well as TRPM3 channels, and the developmental downregulation of Orai1 is consistent with TRP channels being the dominant mechanism in mature astrocytes and oligodendrocytes (Verkhatsky and Parpura 2014). Furthermore, the results show that SOCE is essential for replenishment of intracellular ER Ca^{2+} stores and for the sustainability of ATP-mediated glial Ca^{2+} signalling, which is the primary mechanism of calcium excitability in optic nerve glia (James and Butt 2001). In white matter, ATP-mediated astroglial calcium signalling is triggered by axonal activity (Hamilton et al. 2008), acting to couple the homeostatic and metabolic support functions of glia to axonal activity and metabolic needs (Butt et al. 2014). The present study indicates Orai/Stim and TRPM3 are important elements in the calcium toolkit of optic nerve glia (Fig. 7).

SOCE plays important roles in the sustained phase of glial Ca^{2+} signalling observed following stimulation of G-protein-coupled receptors (GPCR) (Verkhatsky and Parpura 2014). Our results demonstrate SOCE is essential for ATP-mediated Ca^{2+} signalling in optic nerve glia, which has previously been shown to be primarily from IP3-mediated release of Ca^{2+} from intracellular ER stores (Hamilton et al. 2008; James and Butt 2001). As a typical CNS white matter tract, the optic nerve does not contain neuronal somata and the vast bulk of the transcriptome in whole optic nerve extracts represents mRNA from astrocytes and oligodendrocytes (>95%), with minor components from microglia and OPCs (together comprising ~5%), and trace levels from the vasculature and axons (Salter and Fern 2005). qRT-PCR of optic nerve transcripts identified high relative expression of IP3R2, which is consistent with it being the predominant IP3R involved in glial Ca^{2+} signalling (Fiacco and McCarthy 2006; Kanno and Nishizaki 2012). In addition, all three isoforms of Orai were detected by qRT-PCR, together with Stim1 and Stim2. Orai3 is the main microglial CRAC (Ohana et al. 2009), and is also expressed in OPCs (Paez et al. 2007). Our study identified Orai1 and Stim1 in astrocytes, but not Stim2, consistent with a previous report of Orai1/Stim1 forming the main CRAC in cortical astrocytes (Moreno et al. 2012). In contrast, oligodendrocytes were immunopositive for Orai1 and both Stim1 and Stim2, with a suggestion that Stim1 may be localized to the cell somata and Stim2 to the myelin. Interestingly, Golli, a member of the myelin basic protein (MBP) family of proteins has been shown to interact

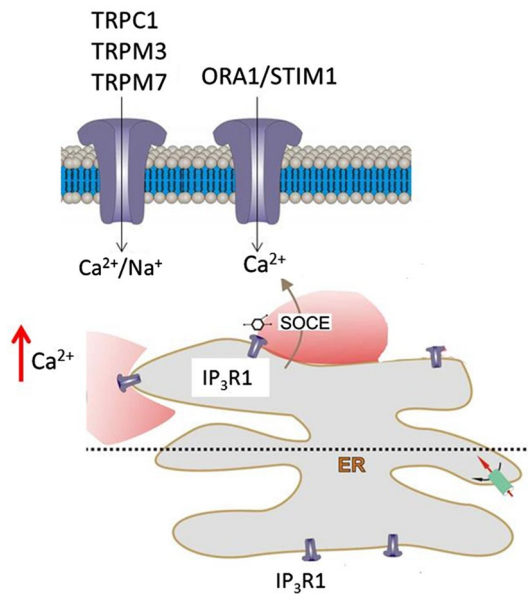


Fig. 7 Mechanisms of SOCE in optic nerve glia. ATP-mediated calcium signalling in optic nerve glia is via P2Y G-protein-coupled receptors and the formation of IP₃, which acts on IP₃R1 on the ER to trigger release of Ca²⁺ into the cytosol. Subsequent replenishment of ER stores in astrocytes and oligodendrocytes is dependent on SOCE via TRPM3 and Orai1, which form the plasmalemmal Ca²⁺ channels, and mainly Stim1, which acts as the sensor of Ca²⁺ depletion, and uptake into the ER is via SERCA pumps. Oligodendrocytes also express Stim2, which may be localized to the myelin, whereas Orai1, Stim1 and TRPM3 are localized to oligodendroglial somata. Notably, calcium homeostasis in optic nerve glia depends on an apparent continuous Ca²⁺ influx from the extracellular milieu that is largely dependent on SOCE. Moreover, SOCE is essential for the sustainability of ATP-mediated Ca²⁺ signalling in optic nerve glia, which has a central role in white matter physiology and pathology

directly with Stim1 (Walsh et al. 2010), and to positively regulate myelin sheet expansion in cultured oligodendrocytes via mechanisms that require Ca²⁺ influx (Paez et al. 2007). In OPCs, the effects of Golli are mediated through the regulation of SOCE (Paez et al. 2009), which involves TRPC1 (Paez et al. 2011). Our findings provide a mechanism by which interactions between oligodendroglial Orai/Stim and Golli control Ca²⁺ influx and the regulation of myelination (Paez et al. 2007), possibly with a predominant role for Stim2 in Ca²⁺ handling specifically within internodal myelin sheaths. Calcium influx in myelin has been demonstrated in response to axonal electrical activity in the optic nerve (Micu et al. 2016), and is required for activity-dependent myelination (Howd et al. 1997) and oligodendroglial metabolic support for electrically active axons (Saab et al. 2016). Moreover, calcium handling is important for axon-myelin maintenance and integrity (Stys 2011), and Ca²⁺-mediated damage is a key feature of ischaemia and multiple sclerosis (Fern et al. 2014).

Interestingly, TRP channels are the main mechanism of SOCE in astrocytes and oligodendrocytes (Verkhatsky and Parpura 2014) and we detected an apparent developmental shift from equal levels of Orai1 and TRPM3 in the postnatal optic nerve to predominantly TRPM3 in the adult. This change corresponds to the major periods of myelination (Dangata et al. 1996) and maturation of astrocyte functions (Reemst et al. 2016), suggesting a potential greater role for Orai/Stim mechanisms of SOCE in immature glia and TRPM3 in mature glia. The most highly expressed TRP channel in the optic nerve was TRPM3, which we showed by immunolabelling is expressed at the protein level in both astrocytes and oligodendrocytes, supporting evidence that the most highly expressed transcripts in optic nerve reflect expression in astrocytes and oligodendrocytes (Salter and Fern 2005). TRPM3 has not previously been demonstrated in astrocytes, but has been identified in oligodendrocytes (Hoffmann et al. 2010), where it is highly localized to the cell somata and hence are most likely the primary molecular basis of SOCE in these cells. The rank order of expression of transcripts detected by qRT-PCR was TRPM3 >> > TRPM7 > TRPC1 > TRPV2 > TRPC3 ≥ TRPM6, with little evidence of developmental regulation between the postnatal and adult optic nerve. The low relative expression of transcripts other than TRPM3 may reflect they are of lesser importance in the predominant cell types, namely astrocytes and oligodendrocytes, and/or are potentially more highly expressed in the minor cell types, namely microglia and OPCs (Salter and Fern 2005). Supporting this, TRPM7 was the second most expressed transcript in the optic nerve and is one of the main TRP channels in microglia (Jiang et al. 2003) and RNA-Seq indicated TRPM7 is the most highly expressed TRP channel transcript in OPCs (Larson et al. 2016). Similarly, transcripts for TRPC1 and TRPC3 were very low in the optic nerve and are implicated, respectively, in OPCs (Paez et al. 2011) and microglia (Mizoguchi et al. 2014). In addition, the low levels of mRNA may reflect low levels of expression in astrocytes, since TRPC1 and TRPV2 are important in astrocytes (Golovina 2005; Parpura et al. 2011; Shibasaki et al. 2013), the latter also being implicated in oligodendrocytes (Fusco et al. 2004), whilst TRPM6 transcripts have been detected in astrocytes of the mouse optic nerve head (Choi et al. 2015). Notably, TRPM6 is central to Mg²⁺ homeostasis (Runnels 2011), and Mg²⁺ deficiency results in hypomyelination in the optic nerve (Gong et al. 2003), raising the possibility that TRPM6 may have an important Mg²⁺ regulatory function in myelination. Transcripts for TRPA1 and TRPV4 were barely detectable in our study, although TRPA1 is linked to astroglial GABA transport (Shigetomi et al. 2011), which is important in the optic nerve (Butt et al. 2014; Howd et al. 1997), and TRPA1 have been implicated in myelin damage

in ischaemia (Hamilton et al. 2016), whilst TRPV4 are implicated in ischaemia in astrocytes (Butenko et al. 2012).

In summary, the results demonstrate SOCE is essential for calcium signalling in optic nerve glia, which has a central role in white matter physiology and pathology, including ischaemia, traumatic injury and multiple sclerosis (Rivera et al. 2016; Butt 2011; Fern et al. 2014). A striking observation is the dependence of glial Ca^{2+} homeostasis on an apparent continuous Ca^{2+} influx from the extracellular milieu, since removal of $[\text{Ca}^{2+}]_o$ resulted in a rapid and marked depletion of $[\text{Ca}^{2+}]_i$ within minutes. The effects of thapsigargin and 2APB, which at high concentrations is a potent inhibitor of Orai and TRP channels (Peinelt et al. 2008; Prakriya and Lewis 2001; Trebak et al. 2002), indicate this is largely dependent on SOCE (Fig. 7). Based on our expression data, the main mechanisms of SOCE are likely to involve TRPM3 and Orai1, which form the plasmalemmal Ca^{2+} channels, and mainly Stim1, which acts as the sensor of Ca^{2+} depletion (Cahalan 2009; Huang et al. 2006; Soboloff et al. 2012). Moreover, TRP channels are permeable to both Ca^{2+} and Na^+ , providing a potential link between glial Ca^{2+} and Na^+ signalling, which together interact to mediate neuronal–glial interactions (Rose and Verkhratsky 2016).

Acknowledgements This research was funded by the Biotechnology and Biological Sciences Research Council (BBSRC), UK, Grant Number BB/J016888 (AB) and the University of Portsmouth Research Development Fund (AL).

Compliance with ethical standards

Conflict of interest The authors declare that they have no conflicts of interest.

All applicable international, national, and/or institutional guidelines for the care and use of animals were followed. All procedures performed in studies involving animals were in accordance with the ethical standards of the institution at which the studies were conducted.

Open Access This article is distributed under the terms of the Creative Commons Attribution 4.0 International License (<http://creativecommons.org/licenses/by/4.0/>), which permits unrestricted use, distribution, and reproduction in any medium, provided you give appropriate credit to the original author(s) and the source, provide a link to the Creative Commons license, and indicate if changes were made.

References

- Abdullaev IF, Bisailon JM, Potier M, Gonzalez JC, Motiani RK, Trebak M (2008) Stim1 and Orai1 mediate CRAC currents and store-operated calcium entry important for endothelial cell proliferation. *Circ Res* 103:1289–1299. doi:10.1161/01.RES.0000338496.95579.56
- Azim K et al (2014) Persistent Wnt/beta-catenin signaling determines dorsalization of the postnatal subventricular zone and neural stem cell specification into oligodendrocytes and glutamatergic neurons. *Stem Cells* 32:1301–1312. doi:10.1002/stem.1639
- Bottenstein JE, Sato GH (1979) Growth of a rat neuroblastoma cell line in serum-free supplemented medium. *Proc Natl Acad Sci USA* 76:514–517
- Brasko C, Hawkins V, De La Rocha IC, Butt AM (2017) Expression of Kir4.1 and Kir5.1 inwardly rectifying potassium channels in oligodendrocytes, the myelinating cells of the CNS. *Brain Struct Funct* 222:41–59. doi:10.1007/s00429-016-1199-8
- Butenko O et al (2012) The increased activity of TRPV4 channel in the astrocytes of the adult rat hippocampus after cerebral hypoxia/ischemia. *PLoS One* 7:e39959. doi:10.1371/journal.pone.0039959
- Butt AM (2011) ATP: a ubiquitous gliotransmitter integrating neuronal–glial networks. *Semin Cell Dev Biol* 22:205–213. doi:10.1016/j.semcdb.2011.02.023
- Butt AM, Fern RF, Matute C (2014) Neurotransmitter signaling in white matter. *Glia* 62:1762–1779. doi:10.1002/glia.22674
- Cahalan MD (2009) STIMulating store-operated Ca^{2+} entry. *Nat Cell Biol* 11:669–677. doi:10.1038/ncb0609-669
- Choi HJ, Sun D, Jakobs TC (2015) Astrocytes in the optic nerve head express putative mechanosensitive channels. *Mol Vis* 21:749–766
- Dangata YY, Findlater GS, Kaufman MH (1996) Postnatal development of the optic nerve in (C57BL × CBA)F1 hybrid mice: general changes in morphometric parameters. *J Anat* 189(Pt 1):117–125
- Fern RF, Matute C, Stys PK (2014) White matter injury: ischemic and nonischemic. *Glia* 62:1780–1789. doi:10.1002/glia.22722
- Fiacco TA, McCarthy KD (2006) Astrocyte calcium elevations: properties, propagation, and effects on brain signaling. *Glia* 54:676–690. doi:10.1002/glia.20396
- Fusco FR et al (2004) Cellular localization of TRPC3 channel in rat brain: preferential distribution to oligodendrocytes. *Neurosci Lett* 365:137–142. doi:10.1016/j.neulet.2004.04.070
- Golovina VA (2005) Visualization of localized store-operated calcium entry in mouse astrocytes. Close proximity to the endoplasmic reticulum. *J Physiol* 564:737–749. doi:10.1113/jphysiol.2005.085035
- Gong H, Takami Y, Amemiya T (2003) Ultrastructure of the optic nerve in magnesium-deficient rats. *Ophthalmic Res* 35:84–92. doi:10.1159/00006913269132
- Greenwood K, Butt AM (2003) Evidence that perinatal and adult NG2-glia are not conventional oligodendrocyte progenitors and do not depend on axons for their survival. *Mol Cell Neurosci* 23:544–558
- Gudz TI, Komuro H, Macklin WB (2006) Glutamate stimulates oligodendrocyte progenitor migration mediated via an alphaV integrin/myelin proteolipid protein complex. *J Neurosci: Off J Soc Neurosci* 26:2458–2466. doi:10.1523/JNEUROSCI.4054-05.2006
- Hamilton N, Vayro S, Kirchhoff F, Verkhratsky A, Robbins J, Gorecki DC, Butt AM (2008) Mechanisms of ATP- and glutamate-mediated calcium signaling in white matter astrocytes. *Glia* 56:734–749. doi:10.1002/glia.20649
- Hamilton NB, Kolodziejczyk K, Kougioumtzidou E, Attwell D (2016) Proton-gated Ca^{2+} -permeable TRP channels damage myelin in conditions mimicking ischaemia. *Nature* 529:523–527. doi:10.1038/nature16519. <http://www.nature.com/nature/journal/v529/n7587/abs/nature16519.html#supplementary-information>
- Hawkins V, Butt A (2013) TASK-1 channels in oligodendrocytes: a role in ischemia mediated disruption. *Neurobiol Dis* 55:87–94. doi:10.1016/j.nbd.2013.03.016
- Hirrlinger PG, Scheller A, Braun C, Quintela-Schneider M, Fuss B, Hirrlinger J, Kirchhoff F (2005) Expression of reef coral fluorescent proteins in the central nervous system of transgenic mice. *Mol Cell Neurosci* 30:291–303 doi:10.1016/j.mcn.2005.08.011

- Hoffmann A et al (2010) TRPM3 is expressed in sphingosine-responsive myelinating oligodendrocytes. *J Neurochem* 114:654–665. doi:[10.1111/j.1471-4159.2010.06644.x](https://doi.org/10.1111/j.1471-4159.2010.06644.x)
- Howd AG, Rattray M, Butt AM (1997) Expression of GABA transporter mRNAs in the developing and adult rat optic nerve. *Neurosci Lett* 235:98–100
- Huang J, Zhang X, McNaughton PA (2006) Modulation of temperature-sensitive TRP channels. *Semin Cell Dev Biol* 17:638–645. doi:[10.1016/j.semcdb.2006.11.002](https://doi.org/10.1016/j.semcdb.2006.11.002)
- James G, Butt AM (2001) P2X and P2Y purinoreceptors mediate ATP-evoked calcium signalling in optic nerve glia in situ. *Cell Calcium* 30:251–259. doi:[10.1054/ceca.2001.0232](https://doi.org/10.1054/ceca.2001.0232)
- Jiang X, Newell EW, Schlichter LC (2003) Regulation of a TRPM7-like current in rat brain microglia. *J Biol Chem* 278:42867–42876. doi:[10.1074/jbc.M304487200](https://doi.org/10.1074/jbc.M304487200)
- Joussset H, Frieden M, Demaurex N (2007) STIM1 knockdown reveals that store-operated Ca^{2+} channels located close to sarco/endoplasmic Ca^{2+} ATPases (SERCA) pumps silently refill the endoplasmic reticulum. *J Biol Chem* 282:11456–11464. doi:[10.1074/jbc.M609551200](https://doi.org/10.1074/jbc.M609551200)
- Kanno T, Nishizaki T (2012) A(2a) adenosine receptor mediates PKA-dependent glutamate release from synaptic-like vesicles and Ca^{2+} efflux from an IP(3)- and ryanodine-insensitive intracellular calcium store in astrocytes. *Cell Physiol Biochem: Int J Exp Cell Physiol Biochem Pharmacol* 30:1398–1412. doi:[10.1159/000343328](https://doi.org/10.1159/000343328)
- Khakh BS, McCarthy KD (2015) Astrocyte calcium signaling: from observations to functions and the challenges therein. *Cold Spring Harbor Perspect Biol* 7:a020404. doi:[10.1101/cshperspect.a020404](https://doi.org/10.1101/cshperspect.a020404)
- Langer J et al (2017) Rapid sodium signaling couples glutamate uptake to breakdown of ATP in perivascular astrocyte endfeet. *Glia* 65:293–308. doi:[10.1002/glia.23092](https://doi.org/10.1002/glia.23092)
- Larson VA, Zhang Y, Bergles DE (2016) Electrophysiological properties of NG2(+) cells: Matching physiological studies with gene expression profiles. *Brain Res* 1638:138–160. doi:[10.1016/j.brainres.2015.09.010](https://doi.org/10.1016/j.brainres.2015.09.010)
- Mandal A, Delamere NA, Shahidullah M (2008) Ouabain-induced stimulation of sodium-hydrogen exchange in rat optic nerve astrocytes. *Am J Physiol Cell Physiol* 295:C100–110. doi:[10.1152/ajpcell.90636.2007](https://doi.org/10.1152/ajpcell.90636.2007)
- Mercer JC, DeHaven WI, Smyth JT, Wedel B, Boyles RR, Bird GS, Putney JW (2006) Large store-operated calcium-selective currents due to co-expression of Orai1 or Orai2 with the intracellular calcium sensor, Stim1. *J Biol Chem* 281:24979–24990. doi:[10.1074/jbc.M604589200](https://doi.org/10.1074/jbc.M604589200)
- Micu I et al (2016) The molecular physiology of the axomyelinic synapse. *Exp Neurol* 276:41–50. doi:[10.1016/j.expneurol.2015.10.006](https://doi.org/10.1016/j.expneurol.2015.10.006)
- Mizoguchi Y et al (2014) Brain-derived neurotrophic factor (BDNF) induces sustained intracellular Ca^{2+} elevation through the up-regulation of surface transient receptor potential 3 (TRPC3) channels in rodent microglia. *J Biol Chem* 289:18549–18555. doi:[10.1074/jbc.M114.555334](https://doi.org/10.1074/jbc.M114.555334)
- Mondragao MA, Schmidt H, Kleinhans C, Langer J, Kafitz KW, Rose CR (2016) Extrusion versus diffusion: mechanisms for recovery from sodium loads in mouse CA1 pyramidal neurons. *J Physiol* 594:5507–5527. doi:[10.1113/JP272431](https://doi.org/10.1113/JP272431)
- Moreno C, Sampieri A, Vivas O, Pena-Segura C, Vaca L (2012) STIM1 and Orai1 mediate thrombin-induced Ca^{2+} influx in rat cortical astrocytes. *Cell Calcium* 52:457–467. doi:[10.1016/j.ceca.2012.08.004](https://doi.org/10.1016/j.ceca.2012.08.004)
- Ohana L, Newell EW, Stanley EF, Schlichter LC (2009) The Ca^{2+} release-activated Ca^{2+} current (I(CRAC)) mediates store-operated Ca^{2+} entry in rat microglia. *Channels (Austin)* 3:129–139
- Paez PM, Spreuer V, Handley V, Feng JM, Campagnoni C, Campagnoni AT (2007) Increased expression of golli myelin basic proteins enhances calcium influx into oligodendroglial cells. *J Neurosci: Off J Soc Neurosci* 27:12690–12699. doi:[10.1523/JNEUROSCI.2381-07.2007](https://doi.org/10.1523/JNEUROSCI.2381-07.2007)
- Paez PM, Fulton DJ, Spreuer V, Handley V, Campagnoni CW, Campagnoni AT (2009) Regulation of store-operated and voltage-operated Ca^{2+} channels in the proliferation and death of oligodendrocyte precursor cells by golli proteins. *ASN Neuro*. doi:[10.1042/AN20090003](https://doi.org/10.1042/AN20090003)
- Paez PM, Fulton D, Spreuer V, Handley V, Campagnoni AT (2011) Modulation of canonical transient receptor potential channel 1 in the proliferation of oligodendrocyte precursor cells by the golli products of the myelin basic protein gene. *J Neurosci: Off J Soc Neurosci* 31:3625–3637. doi:[10.1523/JNEUROSCI.4424-10.2011](https://doi.org/10.1523/JNEUROSCI.4424-10.2011)
- Parpura V, Grubisic V, Verkhratsky A (2011) Ca^{2+} sources for the exocytotic release of glutamate from astrocytes. *Biochim Biophys Acta* 1813:984–991. doi:[10.1016/j.bbamcr.2010.11.006](https://doi.org/10.1016/j.bbamcr.2010.11.006)
- Peinelt C, Lis A, Beck A, Fleig A, Penner R (2008) 2-Aminoethoxydiphenyl borate directly facilitates and indirectly inhibits STIM1-dependent gating of CRAC channels. *J Physiol* 586:3061–3073. doi:[10.1113/jphysiol.2008.151365](https://doi.org/10.1113/jphysiol.2008.151365)
- Pivneva T et al (2008) Store-operated Ca^{2+} entry in astrocytes: differential spatial arrangement of endoplasmic reticulum explains functional diversity in vitro and in situ. *Cell Calcium* 43:591–601. doi:[10.1016/j.ceca.2007.10.004](https://doi.org/10.1016/j.ceca.2007.10.004)
- Prakriya M, Lewis RS (2001) Potentiation and inhibition of Ca^{2+} release-activated Ca^{2+} channels by 2-aminoethyl-diphenyl borate (2-APB) occurs independently of IP(3) receptors. *J Physiol* 536:3–19
- Reemst K, Noctor SC, Lucassen PJ, Hol EM (2016) The indispensable roles of microglia and astrocytes during brain development. *Front Hum Neurosci* 10:566. doi:[10.3389/fnhum.2016.00566](https://doi.org/10.3389/fnhum.2016.00566)
- Rivera A, Vanzulli I, Butt AM (2016) A Central Role for ATP Signaling in Glial Interactions in the CNS. *Curr Drug Targets* 17:1–5. doi:[10.2174/1389450117666160711154529](https://doi.org/10.2174/1389450117666160711154529)
- Rose CR, Verkhratsky A (2016) Principles of sodium homeostasis and sodium signalling in astroglia. *Glia* 64:1611–1627. doi:[10.1002/glia.22964](https://doi.org/10.1002/glia.22964)
- Runnels LW (2011) TRPM6 and TRPM7: a Mul-TRP-PLIK-cation of channel functions. *Curr Pharm Biotechnol* 12:42–53
- Saab AS et al (2016) Oligodendroglial NMDA receptors regulate glucose import and axonal energy metabolism. *Neuron* 91:119–132. doi:[10.1016/j.neuron.2016.05.016](https://doi.org/10.1016/j.neuron.2016.05.016)
- Salter MG, Fern R (2005) NMDA receptors are expressed in developing oligodendrocyte processes and mediate injury. *Nature* 438:1167–1171. doi:[10.1038/nature04301](https://doi.org/10.1038/nature04301)
- Shibasaki K, Ishizaki Y, Mandadi S (2013) Astrocytes express functional TRPV2 ion channels. *Biochem Biophys Res Commun* 441:327–332. doi:[10.1016/j.bbrc.2013.10.046](https://doi.org/10.1016/j.bbrc.2013.10.046)
- Shigetomi E, Tong X, Kwan KY, Corey DP, Khakh BS (2011) TRPA1 channels regulate astrocyte resting calcium and inhibitory synapse efficacy through GAT-3. *Nat Neurosci* 15:70–80. doi:[10.1038/nn.3000](https://doi.org/10.1038/nn.3000)
- Simpson PB, Russell JT (1997) Role of sarcoplasmic/endoplasmic reticulum Ca^{2+} -ATPases in mediating Ca^{2+} waves and local Ca^{2+} -release microdomains in cultured glia. *Biochem J* 325(Pt 1):239–247
- Singaravelu K, Lohr C, Deitmer JW (2006) Regulation of store-operated calcium entry by calcium-independent phospholipase A2 in rat cerebellar astrocytes. *J Neurosci: Off J Soc Neurosci* 26:9579–9592. doi:[10.1523/JNEUROSCI.2604-06.2006](https://doi.org/10.1523/JNEUROSCI.2604-06.2006)
- Soboloff J, Rothberg BS, Madesh M, Gill DL (2012) STIM proteins: dynamic calcium signal transducers. *Nat Rev Mol Cell Biol* 13:549–565. doi:[10.1038/nrm3414](https://doi.org/10.1038/nrm3414)

- Stys PK (2011) The axo-myelinic synapse. *Trends Neurosci* 34:393–400. doi:[10.1016/j.tins.2011.06.004](https://doi.org/10.1016/j.tins.2011.06.004)
- Trebak M, Bird GS, McKay RR, Putney JW Jr (2002) Comparison of human TRPC3 channels in receptor-activated and store-operated modes. Differential sensitivity to channel blockers suggests fundamental differences in channel composition. *J Biol Chem* 277:21617–21623. doi:[10.1074/jbc.M202549200](https://doi.org/10.1074/jbc.M202549200)
- Verkhatsky A, Parpura V (2014) Store-operated calcium entry in neuroglia. *Neurosci Bull* 30:125–133. doi:[10.1007/s12264-013-1343-x](https://doi.org/10.1007/s12264-013-1343-x)
- Walsh CM, Doherty MK, Tepikin AV, Burgoyne RD (2010) Evidence for an interaction between Golgi and STIM1 in store-operated calcium entry. *Biochem J* 430:453–460. doi:[10.1042/bj20100650](https://doi.org/10.1042/bj20100650)